


Solution NMR Approaches for Establishing Specificity of Weak Heterodimerization of Membrane Proteins

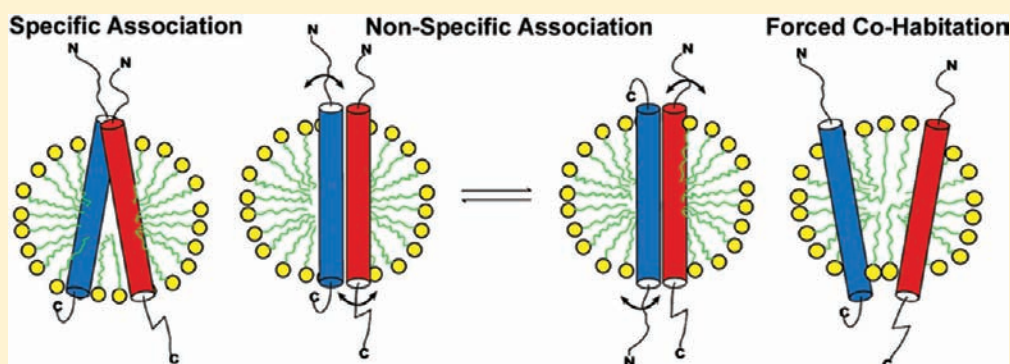
Tiandi Zhuang,[†] Bing K. Jap,[‡] and Charles R. Sanders^{*,†}

[†]Department of Biochemistry and Center for Structural Biology, Vanderbilt University School of Medicine, Nashville, Tennessee 37232, United States

[‡]Life Sciences Division, Lawrence Berkeley National Laboratory, Berkeley, California 94720, United States

 Supporting Information

ABSTRACT:



Solution NMR provides a powerful approach for detecting complex formation involving weak to moderate intermolecular affinity. However, solution NMR has only rarely been used to detect complex formation between two membrane proteins in model membranes. The impact of *specific binding* on the NMR spectrum of a membrane protein can be difficult to distinguish from spectral changes that are induced by *nonspecific binding* and/or by changes that arise from *forced cohabitation* of the two proteins in a single model membrane assembly. This is particularly the case when solubility limits make it impossible to complete a titration to the point of near saturation of complex formation. In this work experiments are presented that provide the basis for establishing whether specific complex formation occurs between two membrane proteins under conditions where binding is not of high avidity. Application of these methods led to the conclusion that the membrane protein CD147 (also known as EMMPRIN or basigin) forms a specific heterodimeric complex in the membrane with the 99-residue transmembrane C-terminal fragment of the amyloid precursor protein (C99 or APP- β CTF), the latter being the immediate precursor of the amyloid- β polypeptides that are closely linked to the etiology of Alzheimer's disease.

INTRODUCTION

Because NMR chemical shifts for any given compound are often very sensitive to the local molecular environment, NMR methods represent a powerful approach for detecting complex formation between two molecules in solution. This has proven especially important for the case of pairs of biomolecules that form specific complexes with only low to moderate affinity. For such complexes the on/off rates for complex formation and dissociation are usually rapid on the NMR time scale, such that observed chemical shifts represent the population-weighted averages between the intrinsic spectra of free and complex species. Assuming rapid exchange on the NMR time scale and that "molecule A" can be titrated with "molecule B" from 0% saturation of molecule A to near saturation, the changes induced in the spectrum of molecule A can be quantitated as a function of the concentration of molecule B to confirm specificity of complex formation and to determine the dissociation constant, which

reflects the free energy difference between free and complexed states. Use of NMR often confers an added advantage in that the nature of the changes observed between the free and complexed state spectra sometimes provides direct insight into the structure and dynamics of the complex. For example, NMR has been used to map the binding interface between two membrane-associated molecules.^{1–5}

Complex formation between integral membrane proteins in bilayers or in model membranes such as detergent micelles can be difficult to detect, particularly when affinity is modest such that complexes do not have lifetimes of sufficient duration to allow them to be "trapped" using chemical or biochemical methods (such as pull-down assays). NMR can sometimes be used to monitor titration of one molecule with the other.

Received: September 29, 2011

Published: November 15, 2011

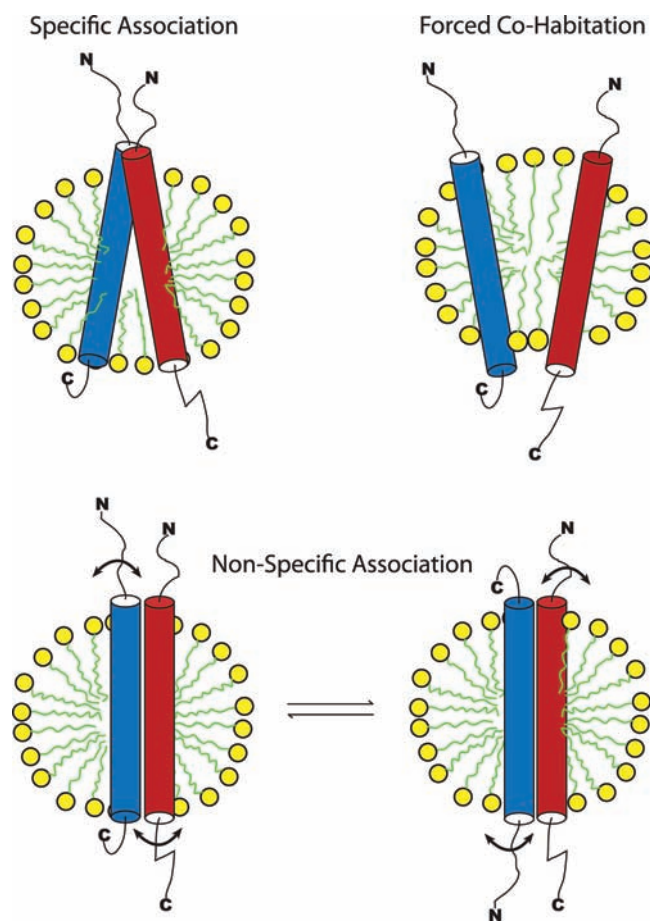


Figure 1. Possible modes of interactions of two membrane proteins in model membranes. Detergent micelles are shown, but the same principles apply to other classes of model membranes. (Top left) Specific association. (Top right) Forced cohabitation. Two membrane proteins with no affinity for each other are forced to share a single model membrane unit by statistical mechanics and/or because the number of membrane protein molecules exceeds the number of available model membrane units present in the solution. (Bottom) Nonspecific association. By way of example, we have depicted two exchanging modes of transient 1:1 association in which the interaction interfaces are not fixed but are heterogeneous (indicated by the motion arrows). Many other possible modes of interaction and non-1:1 stoichiometries would also fit into this class.

However, when affinity is only modest, it can sometimes be difficult to carry out the titration to the point of near saturation before the solubility limit of the titrant is reached. In this case, changes are observed in the spectrum of “protein A” during titration by “protein B”, but the shift vs B concentration curves may be nearly linear. In such cases, it is unclear whether the observed shifts represent specific formation of a stoichiometric complex or whether the shifts result from nonspecific binding or forced cohabitation of two proteins in a single model membrane unit (e.g., a detergent micelle) (Figure 1). *Specific association* is here defined as stoichiometric complex formation that involves a specific intermolecular interface. *Nonspecific association* means that there is affinity between molecules, but that this affinity does not lead to formation of complexes of specific stoichiometry involving structurally well-defined intermolecular interfaces. An example is provided by “promiscuous inhibitors”, colloidal aggregates of druglike molecules that will form complexes with

many different proteins, mostly via hydrophobic interactions.⁶ *Forced cohabitation* means the entrapment of two hydrophobic molecules in the same micelle simply because there are not enough micelles present to allow all of the hydrophobic molecules to populate their own micelles.⁷ While the two molecules may have no affinity for each other, they may nevertheless be forced to interact by virtue of coentrapment in a very small space (i.e., within the same detergent micelle). In all three cases, intermolecular interactions may be NMR-detectable. Here, we developed an approach to distinguish between these possibilities.

As a test case for the approach being developed in this study, we examined interactions between two single-span membrane proteins: the C-terminal 99 residue transmembrane domain of the amyloid precursor protein (C99, also known as APP- β CTF) and the C-terminal transmembrane and cytosolic domains of CD147 (see Figure 2A). C99 is a very important protein, serving as the immediate precursor for the amyloid- β ($A\beta$) polypeptides that are widely believed to be central to the etiology of Alzheimer’s disease. CD147 (also known as EMMPRIN or basigin) is a protein that has been shown to reduce levels of amyloid- β under cellular conditions,^{8–10} a potentially beneficial activity in the sense that such activity could disfavor Alzheimer’s disease. However, the mechanism by which CD147 lowers $A\beta$ production remains unclear. Full-length CD147 is a 27 kDa cell surface protein with two extracellular N-terminal immunoglobulin domains, a single transmembrane segment, and a small intracellular domain (Figure 2A).¹¹ The obviation of CD147 by RNA interference causes dose-dependent increases in the levels of secreted $A\beta$.^{8,10} Although CD147 was coimmunoprecipitated with the γ -secretase complex that cleaves C99 to release $A\beta$,¹² and observed to copurify with γ -secretase,¹³ additional studies suggested that any direct CD147 association with γ -secretase is transient.¹³ Moreover, CD147 expression had no effects on the expression and stability of γ -secretase core subunits^{8,10} or on the association of the γ -secretase complex with lipid rafts.⁸ On the basis of these observations, it was suggested that CD147 does not directly modulate γ -secretase cleavage of APP and that the decrease in $A\beta$ levels induced by CD147 might be due to stimulation of expression of an as yet to be identified matrix metalloprotease.⁸ This hypothesis does not preclude the possibility that the amyloid- β lowering activity of CD147 might involve direct association with APP or C99. The work described in this paper provides a direct test for complex formation between C99 and the transmembrane/cytosolic C-terminal domain of CD147 (CD147-CTD).

Finally, we note that a complication to this study is the fact that the transmembrane domain of C99 contains GXXXG motifs that confer a propensity for homodimerization.^{1,14,15} Accordingly, in developing methods for testing for specific heterodimerization of C99 with CD147-CTD, we have to consider the possibility that homodimerization of C99 may compete with this process.

RESULTS

Expression and Purification of the Transmembrane/Cytosolic Domain of CD147. Human CD147-CTD (Figure 2A) was expressed in *Escherichia coli* and then purified into lysomyristoylphosphatidylglycerol (LMPG) micelles, a detergent that we have previously shown to be well-suited for NMR studies of C99.¹ The purity of the 10 kDa protein was confirmed with sodium dodecyl sulfate–polyacrylamide gel electrophoresis (SDS–PAGE; Figure 2B). Far-UV CD (circular dichroism)

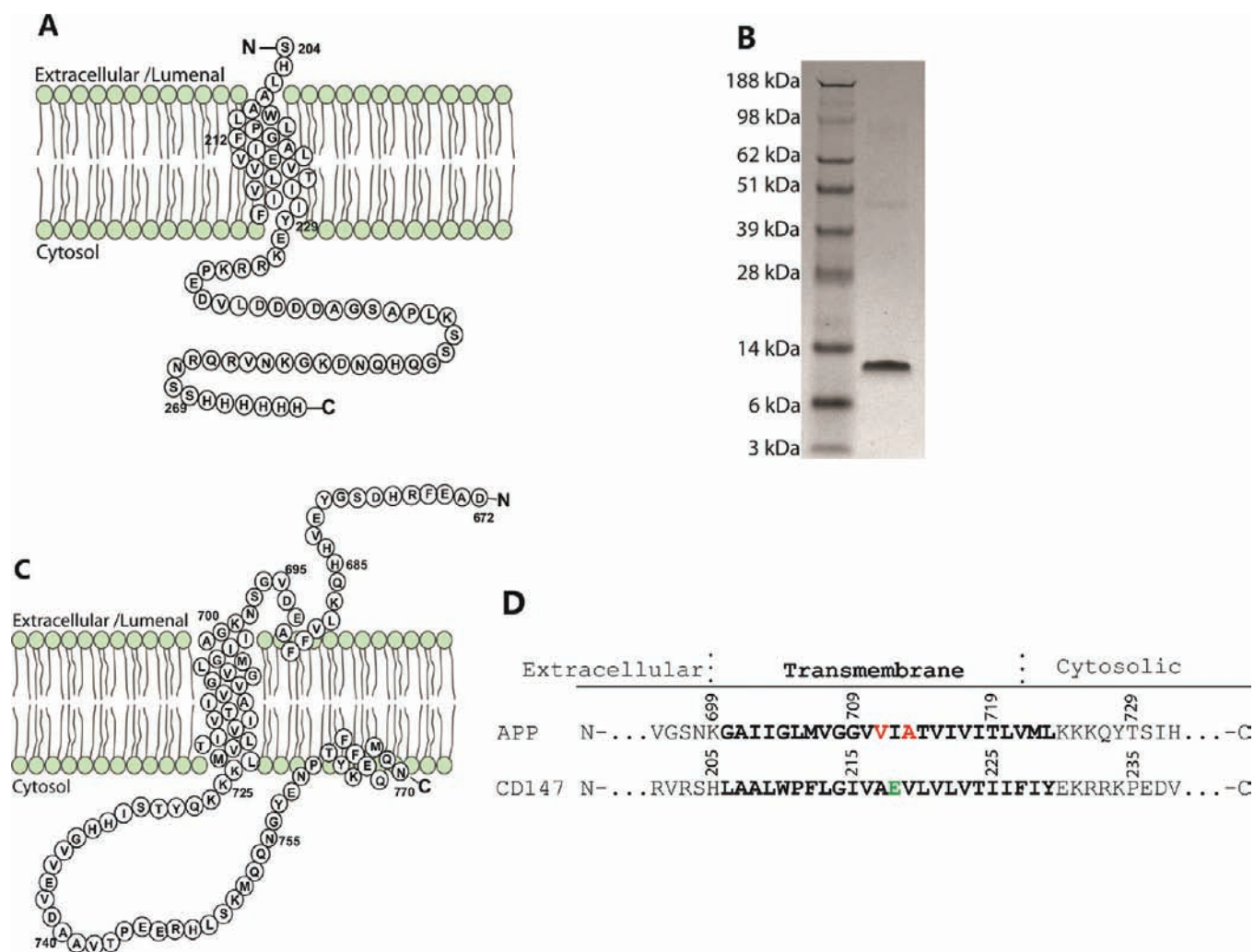


Figure 2. (A) Sequence and topology plot for the CD147 transmembrane/cytosolic domain. (B) SDS-PAGE gel with Coomassie staining of the purified CD147-CTD. (C) Sequence and topology plot for C99. (D) Sequence alignments for the transmembrane domains of human C99 and human CD147-CTD. The γ -secretase cleavage sites at C99 for production of $A\beta_{40}$ and $A\beta_{42}$ are highlighted in red. The unusual glutamic acid in the CD147 transmembrane domain is highlighted in green. The transmembrane sequence of CD147 is highly conserved among all species.

spectroscopy (not shown) indicated that CD147-CTD is a mostly helical protein in LMPG micelles, consistent with the fact that CD147 is a type I integral membrane protein. It was found that lowering the solution pH below 7.4 resulted in significantly reduced solubility, so the experiments described in this paper were carried out at pH 7.4. At this pH and in LMPG micelles, C99 yields a much better NMR spectrum than CD147-CTD (not shown). Accordingly, studies of interactions between C99 and CD147-CTD were conducted by monitoring the ^1H - ^{15}N TROSY (transverse relaxation optimized spectroscopy) NMR spectrum of uniformly ^{15}N -labeled C99, with the unlabeled CD147-CTD being spectroscopically silent. In previous studies near-complete amide ^1H - ^{15}N resonance assignments of $[\text{U}-^{15}\text{N}]$ C99 in LMPG were determined¹ at pH 6.5. For this work it was possible to directly correlate a number of the peaks from the pH 6.5 TROSY spectrum to the corresponding peaks in the pH 7.4 spectrum, permitting assignment of the latter, as shown in Figure 3.

Complex Formation between C99 and CD147-CTD Is Not Detected at Low Protein Mole Fractions in the Micelles. NMR has been widely used to map ligand binding interfaces of

proteins by monitoring titration-induced NMR peak chemical shift changes or intensity variations.¹⁶ For the titrations of this work it is important to consider the thermodynamic nature of the protein concentration in a membrane-mimetic environment (i.e., detergent micelles). For molecular association occurring in model membranes, bulk concentration units are not thermodynamically appropriate.^{17,18} Instead, mole fraction percentage units should be used. For example, while the bulk concentration of a 1 mM membrane protein is the same whether the sample contains 100 or 200 mM detergent, from a thermodynamic standpoint the “interfacial concentration” of the protein is twice as high in 100 mM detergent (ca. 1 mol %) as in 200 mM detergent (ca. 0.5 mol %).

We monitored the ^1H - ^{15}N TROSY spectrum from 0.2 mM $[\text{U}-^{15}\text{N}]$ C99 as it was titrated with unlabeled CD147-CTD to test whether direct association of these proteins can be detected under conditions of a high (190 mM, 9%) and constant LMPG concentration, conditions in which the mole fraction of C99 in the micelles is low such that little homodimer is present (see below). As a negative control, we also titrated $[\text{U}-^{15}\text{N}]$ C99 with unlabeled KCNE1, a single-span membrane protein that

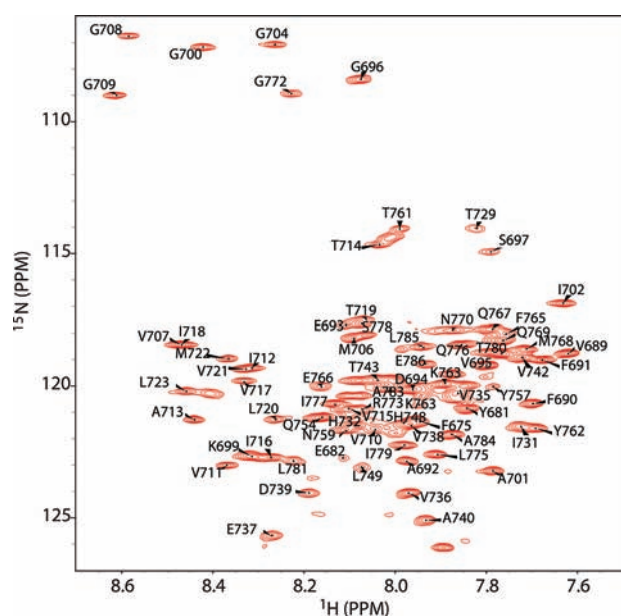


Figure 3. ^1H – ^{15}N TROSY (600 MHz) spectrum of C99 in 2.5% (w/v) LMPG micelles acquired at 45 °C. The pH of the sample was 7.4. The resonances were assigned by tracing the resonance chemical shift changes through a series of pH titration experiments between pH 6.5 and pH 7.5. The ^1H – ^{15}N TROSY spectrum of C99 was previously assigned at pH 6.5.¹

modulates potassium channel function^{19,20} and that appears to be completely unrelated to C99 and CD147 and their associated cell biology. Figure 4 shows the results for these experiments. No chemical shift changes were observed in the spectra of C99 even after addition of a 4-fold molar excess of either CD147-CTD or KCNE1. We conclude that under very dilute conditions (only 0.1 mol % C99 in the membrane-mimetic phase) no direct interaction between CD147-CTD and C99 can be detected.

Interaction of C99 with CD147-CTD Is Evident at Higher Protein Mole Fractions in the Micelles. To examine the detergent effect on possible heterodimerization of CD147-CTD with 0.2 mM C99, we repeated titration experiments at 2.5% (50 mM) LMPG, conditions in which the C99 concentration is 0.4 mol %. Significant CD147-CTD-induced chemical shift changes were observed in the ^1H – ^{15}N TROSY NMR spectrum of $[\text{U}-^{15}\text{N}]\text{C99}$ as shown in Figure 5A (see also site-specific shifts in Supporting Figure 2, Supporting Information). The assignable peaks that exhibited the largest chemical shift changes are located primarily within the transmembrane or juxtamembrane domains. Significant chemical shift perturbations were also observed for residues V689 and F690, which are located in a membrane surface-penetrating amphipathic helix on the N-terminus.¹ However, no chemical shift changes in C99's spectrum were observed upon negative control titration of KCNE1 under identical conditions in 2.5% LMPG, as shown in Figure 5B. These results suggest C99 undergoes heterodimerization with CD147 (but not with KCNE1) at higher mole percent concentrations of the proteins in the model membranes. The plot of chemical shift changes versus the mole percent of CD147-CTD appears to exhibit the beginning of hyperbolic curvature (Supporting Figure 2), which suggests their binding is specific. However, the avidity of association between C99 and CD147-CTD appears to be modest as evidenced by the fact that

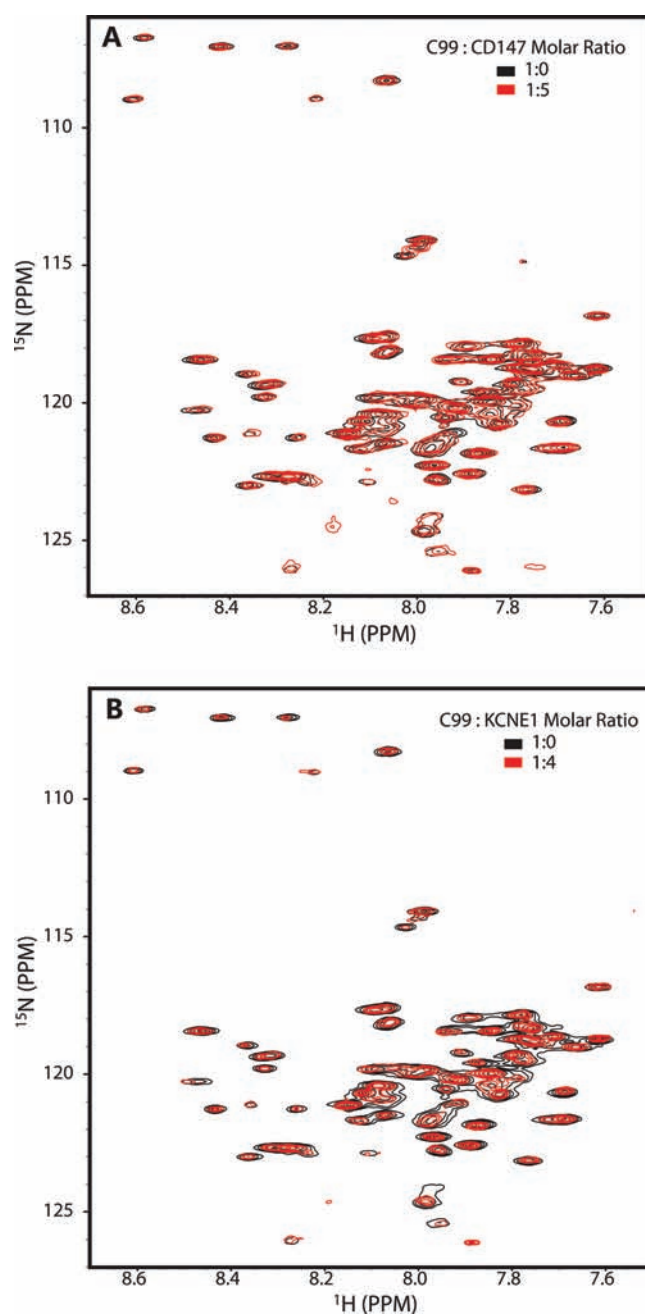


Figure 4. Titrations of 0.2 mM (0.11 mol %) $[\text{U}-^{15}\text{N}]\text{C99}$ with either unlabeled CD147-CTD (A) or unlabeled KCNE1 (negative control, B) at high detergent concentration as monitored by 600 MHz ^1H – ^{15}N TROSY NMR spectra at 45 °C. The sample buffer in both cases contained 250 mM imidazole and 9% LMPG (188 mM), pH 7.4.

saturation was not approached even upon reaching a 4-fold molar excess of CD147-CTD over C99 in the titration.

To further test how the detergent concentration affects the heterodimerization, C99 and CD147-CTD were mixed at constant concentrations (0.2 and 1 mM, respectively) and NMR spectra for $[\text{U}-^{15}\text{N}]\text{C99}$ were collected as the LMPG concentration was varied from 2.2% to 9%. (The high LMPG concentration in the CD147-CTD protein stock solution made it impossible to generate samples with LMPG concentrations lower than 2.2%.) Even though this range of accessible LMPG

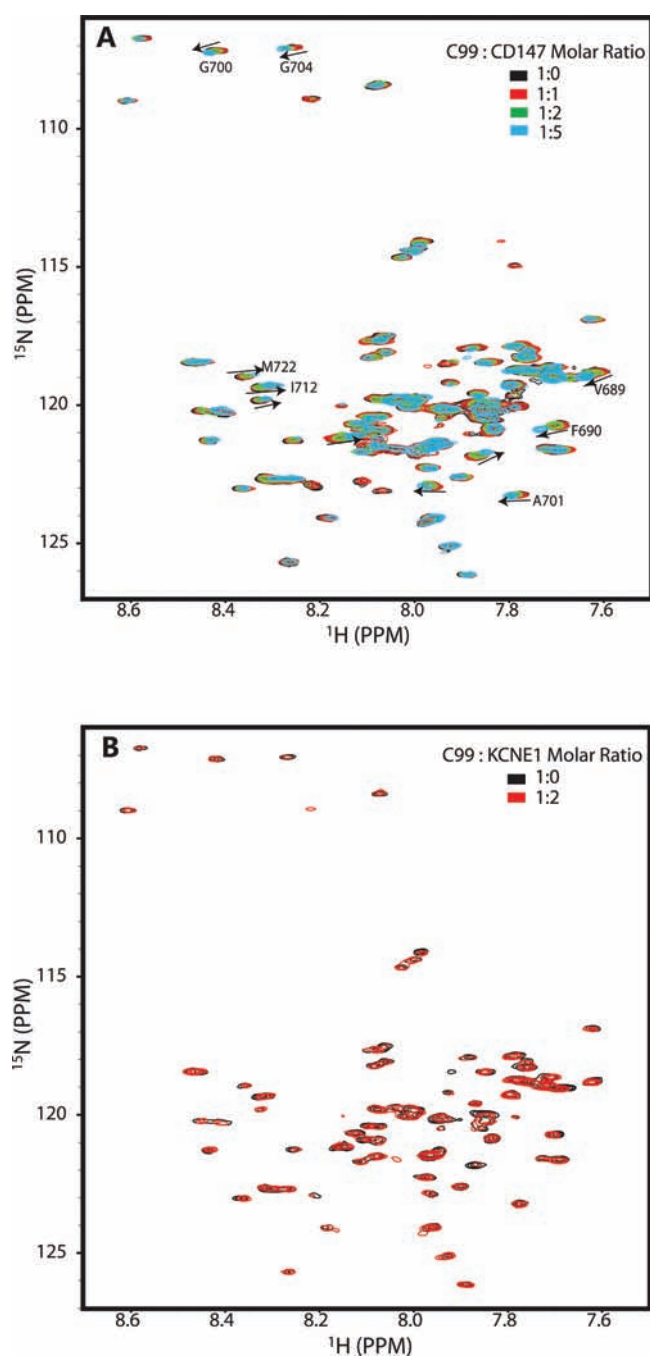


Figure 5. Titrations of 0.2 mM (0.4 mol %) [U- ^{15}N]C99 with either unlabeled CD147-CTD (A) or unlabeled KCNE1 (negative control, B) at moderate detergent concentration as monitored by 600 MHz ^1H - ^{15}N TROSY NMR spectra at 318 K. The sample buffer in both cases contained 250 mM imidazole and 2.5% LMPG (52 mM), pH 7.4. Site-specific changes in chemical shifts observed over the course of the CD147-CTD titration are presented as a bar graph in Supporting Figure 2 in the Supporting Information.

concentration is modest, significant LMPG concentration-dependent chemical shift changes were observed (Figure 6; see also site-specific shifts in Supporting Figure 3, Supporting Information). Resonances exhibiting the largest chemical shift changes generally match those shown in Figure 5A (compare also Supporting Figures 2 and 3) and reflect a shift in the

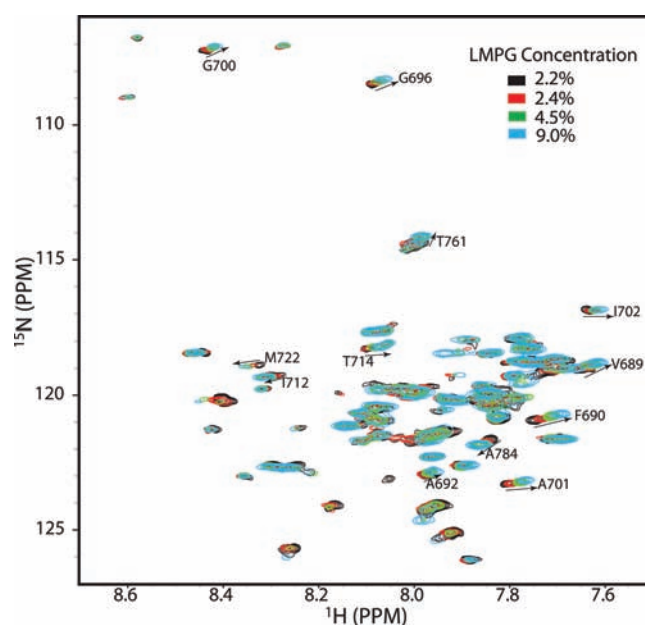


Figure 6. ^1H - ^{15}N TROSY (600 MHz) spectra of 0.2 mM [U- ^{15}N]C99 plus 1 mM unlabeled CD147-CTD at varying weight % concentrations of LMPG (2.2%, black; 2.4%, red; 4.5%, green; 9.0%, cyan) at 45 °C. The buffer contained 250 mM imidazole, pH 7.4. Site-specific changes in chemical shifts observed over the course of this titration are presented as a bar graph in Supporting Figure 3 in the Supporting Information.

monomer–heterodimer equilibrium toward monomer at the higher LMPG concentrations. This supports the notion that heterodimerization is taking place at higher protein concentrations in the mixed micelles. That dimerization reflects the specific avidity of C99 and CD147-CTD for each other and not just the consequence of forcing these two molecules to cohabitate the same micelles is supported by the fact that a 2× molar excess of the negative control KCNE1 protein does not perturb C99’s spectrum, even at the lower LMPG concentrations (Figure 5B).

Homodimerization of C99 Can Also Be Detected at Higher Mole Fractions in Micelles. There is a variety of evidence that C99 or its derived transmembrane fragment forms homodimers under membrane or model membrane conditions.^{1,14,21–25} Here we examined the avidity and reversibility of C99 homodimerization by acquiring ^1H - ^{15}N TROSY spectra of 0.2 mM [U- ^{15}N]C99 as the LMPG concentration was varied over a range of concentrations: 0.7%, 2.0%, 4.5%, and 10% (15–210 mM) LMPG. As expected, significant chemical shift changes were observed, which is likely due to a shift in the monomer–dimer equilibrium toward the monomer at higher LMPG concentrations. Interestingly, the peaks exhibiting the largest chemical shift changes (Figure 7; Supporting Figure 4, Supporting Information) exhibited some modest degree of overlap with those observed to shift the most in response to titration by CD147-CTD (Figure 5 and Supporting Figure 2). This suggests that the location of the homodimerization interface on C99 overlaps with that involved in heterodimerization with CD147. However, the directions of the shift changes for these most affected peaks were sometimes different for the C99-only titration relative to those of their corresponding responses to titration by CD147-CTD. This reflects the chemically distinct nature of the interface for the homodimer versus the heterodimer. As in the case of heterodimerization, shift versus C99 protein concentration curves did

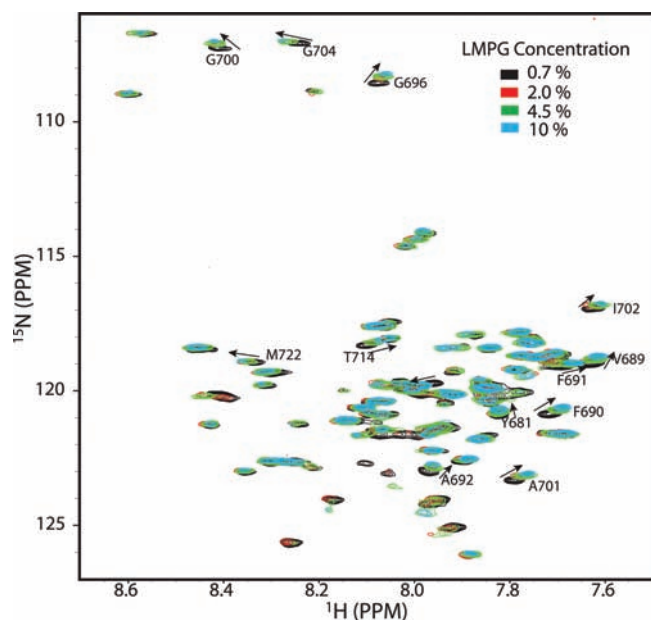


Figure 7. ^1H – ^{15}N TROSY (600 MHz) spectra of 0.2 mM $[\text{U}-^{15}\text{N}]$ C99 at varying weight % concentrations of LMPG (0.7%, black; 2.0%, red; 4.5%, green; 10%, cyan) at 45 °C. The buffer contained 250 mM imidazole, pH 7.4. Site-specific changes in chemical shifts observed over the course of this titration are presented as a bar graph in Supporting Figure 4 in the Supporting Information.

not exhibit saturation at high protein-to-detergent ratios (Supporting Figure 4), indicating that conversion to homodimer remains incomplete even at the highest accessible C99 mole fraction concentration. Evidently, homodimerization, like heterodimerization, is not very avid in LMPG micelles. These data also indicate that heterodimerization of C99 with CD147-CTD is more favorable than C99 homodimerization since the CD147-induced chemical shift changes “override” the homodimerization-induced chemical shift changes seen when the detergent concentration is varied in the C99-only case.

Paramagnetic Relaxation Enhancement (PRE) Measurements Verify Specific Complex Formation between CD147-CTD and C99. PRE NMR experiments have received increasing application as a route to long-range distance information (up to 25 Å) for use in structure determination or refinement.^{26,27} Distances between a spin label fixed at a site in a protein and NMR-active nuclei in the protein (usually amide ^1H) can be extracted from the paramagnet-induced increased NMR transverse relaxation rates, manifested as line broadening. Spin labels placed on proteins have also been used to screen for the binding of small molecules on the basis that PRE from a spin label on the protein will result in dramatic line broadening in the spectra of small molecules that bind to proximal sites on the protein, provided that on/off exchange is rapid on the NMR time scale.^{27–29} This approach was adapted for our study of heterodimerization between C99 and CD147-CTD. Two different single-cysteine forms of CD147-CTD were prepared (F212C and Y229C). Each was then spin labeled at their cysteine sites using the thiol-reactive nitroxide reagent MTS (2,2,5,5-tetramethyl-3-pyrrolyl-3-methyl methanethiosulfonate). To address the relative protein orientations during heterodimerization, one cysteine mutant (F212C) was introduced into the transmembrane domain of CD147-CTD close to the extracellular interface (see Figure 2A).

The other spin label was attached to a site (Y229C) also located in the transmembrane segment, but close to the cytosolic domain. For use as a negative control, spin-labeled KCNE1 was prepared using a single-cysteine mutant form of this protein (S64C on the juxtamembrane segment close to the cytoplasmic domain).

To 0.2 mM $[\text{U}-^{15}\text{N}]$ C99 in 2.5% LMPG was added spin-labeled CD147-CTD or KCNE1. ^1H – ^{15}N TROSY spectra were recorded under both paramagnetic and diamagnetic conditions. The reductions in peak intensities resulting from paramagnetic relaxation enhancement-based line broadening are shown in Figure 8. For titrations of C99 by both spin-labeled CD147-CTD and spin-labeled KCNE1 (negative control), widespread peak broadening in the spectrum of $[\text{U}-^{15}\text{N}]$ C99 was evident. However, the line broadening induced by spin-labeled KCNE1 was observed to be rather uniform throughout the spectrum (Figure 8C; Supporting Figure 5, Supporting Information), indicating that while KCNE1 and C99 may cohabitate the same micelle, which forces them to be in close proximity, there is no preferred mode of interaction that reflects complex formation. However, in the cases of spin-labeled Y229C and F212C mutant forms of CD147-CTD, we observed nonuniform line broadening in C99’s NMR spectrum. Spin-labeled F212C-CD147-CTD induced the greatest degree of line broadening in the ^1H – ^{15}N TROSY resonances from C99 residues in the 689–709 range, sites located in the extracellularly disposed juxtamembrane or transmembrane domains (Figure 8B). In the case of spin-labeled Y229C-CD147-CTD, only residues located in the cytosolic C-terminus exhibited significant line broadening beyond the average (Figure 8A and Supporting Figure 5A). Combined with the earlier observation that the peaks exhibiting the largest chemical shift changes in the spectrum of C99 in response to homodimerization are largely the same set of C99 peaks that shift in response to heterodimerization with CD147-CTD, these results confirm that C99 and CD147-CTD form a specific heterodimeric complex that involves largely the same set of C99 residues that are also involved in homodimerization of this protein. This dimer interface on C99 includes both sites located in the short amphipathic helix (residues 689–692) found just before the start of the transmembrane domain and also glycine residues that are part of tandem GXXXG motifs found in the extracellular end of the transmembrane domain (see Figure 1C).

DISCUSSION

Distinguishing between Specific Association, Nonspecific Association, and Forced Cohabitation under Micellar Conditions. The experiments described in this work establish a general approach that can be used to classify interactions occurring between a pair of membrane proteins as being the consequence of specific association, nonspecific association, or forced cohabitation of two proteins of the same model membrane units (Figure 1). The first of these experiments was to carry out a pair of ^1H – ^{15}N TROSY-monitored titrations of protein A (i.e., C99) with both its potential partner, protein B (i.e., CD147-CTD), and with a negative control membrane protein (i.e., KCNE1) that has the same membrane topology as protein B, but that should have no affinity for protein A. In this work it was seen that at higher protein-to-detergent ratios the negative control protein KCNE1 induced essentially no shifts in the spectrum of C99, a result very different from what was seen when C99 was titrated by CD147-CTD. This eliminated the possibility that the CD147-CTD-induced shifts were due to

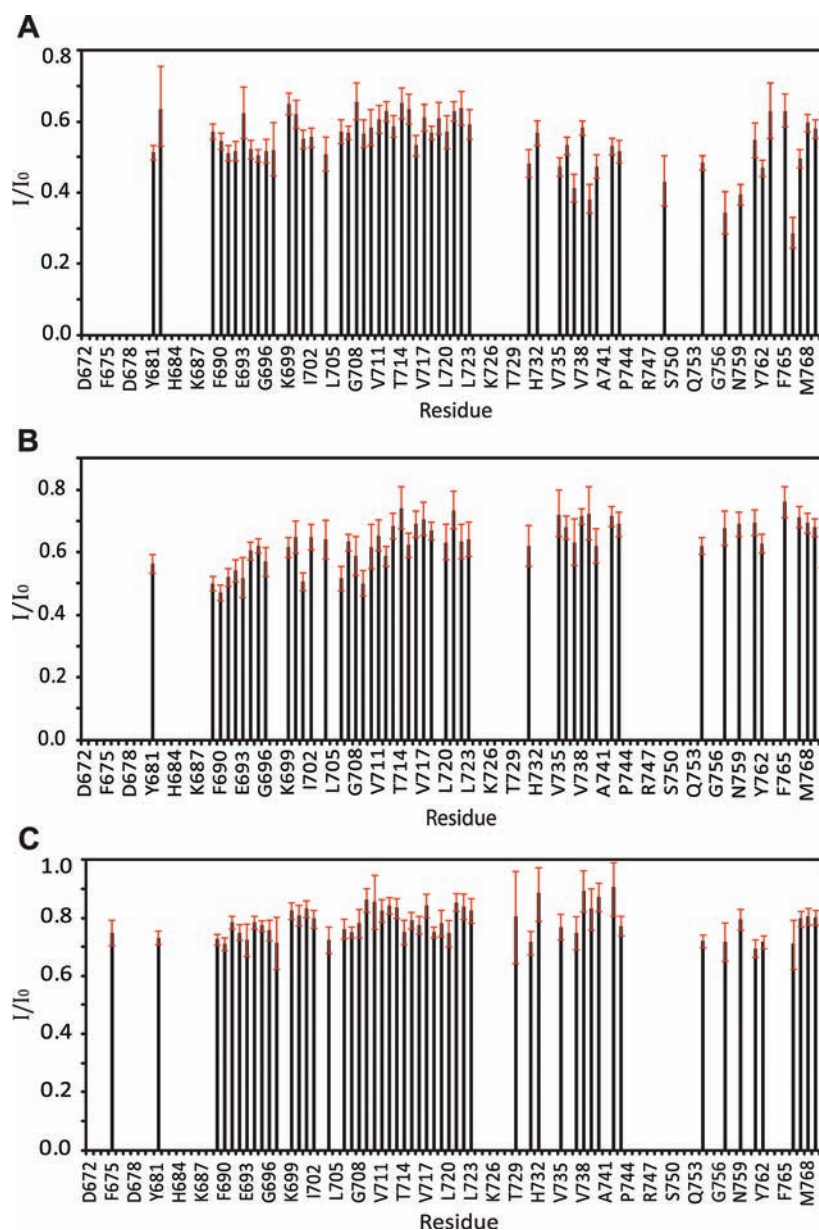


Figure 8. Site-specific PRE reductions in the intensities of 600 MHz $^1\text{H}-^{15}\text{N}$ TROSY peaks from 0.2 mM $[\text{U}-^{15}\text{N}]\text{C99}$ resulting from the presence of (A) a 4× molar excess of nitroxide spin-labeled Y229C CD147-CTD, (B) a 4× molar excess of nitroxide spin-labeled F212C CD147-CTD, or (C) a 2× molar excess of nitroxide spin-labeled S64C KCNE1. I/I_0 values represent the difference between C99 TROSY peak heights in the presence of either spin-labeled CD147-CTD or spin-labeled KCNE1 relative to the corresponding C99 peak intensities (which are higher) under diamagnetic conditions (see the Methods for additional information). All samples contained 2.5% LMPG at pH 7.4, with the NMR data being acquired at 45 °C. The residues for which measurements are not reported represent those with unassigned or unresolved peaks.

forced cohabitation of protein CD147-CTD and C99 in the same micelle. The approach used to reach this conclusion should be generally applicable, with judicious choice and preparation of a suitable membrane protein for use as the negative control being essential. We note that, thanks to recently developed structural genomics repositories and other resources (cf. <http://psimr.asu.edu>), *E. coli* expression systems are now available for numerous membrane proteins, facilitating choice and access to a suitable negative control membrane protein.

The second set of experiments introduced in this work allowed specific binding to be distinguished from nonspecific binding. This experiment requires that protein B (i.e., CD147-CTD) be

prepared in two different spin-labeled forms—one with the spin label at or near the extracellular domain and one with the spin label at or near the cytosolic domain. If specific binding is taking place, then when these spin-labeled forms of protein B are titrated into a protein A solution, the amide sites on protein A for which TROSY/HSQC peaks are most profoundly broadened should be those that are located on the same side of the native membrane as the spin-labeled site in protein B. On the other hand, titration of membrane protein A with a spin-labeled negative control membrane protein should reveal patterns of line broadening in the spectrum of protein A that reflect only nonspecific interactions. For example, if the spin label is located

on the extracellular domain of the negative control protein, roughly equal broadening should be observed in peaks from both the extra- and intracellular domains of protein A. In this work we used these experiments to confirm that the interactions of C99 and CD147-CTD involve specific association, whereas the interaction between C99 and KCNE1 was seen to be of a nonspecific nature.

The two sets of experiments introduced in this work provide only qualitative insight into affinity. Quantitation of K_d would require that other (possibly non-NMR) methods be used. However, qualitative insight is not inconsequential. Here we found that binding could not readily be detected via chemical shift perturbation when the C99 and CD147 concentrations were on the order of 0.1 mol %, but could be detected at a ≥ 4 -fold higher concentration, where changes in the NMR spectrum of C99 are roughly linear with CD147-CTD concentrations up to 2 mol %. This indicates that K_d for these two proteins in LMPG micelles must be ≥ 2 mol %.

A final set of experiments that proved very useful in this work was to monitor the NMR spectrum of C99-only as a function of the protein-to-detergent ratio. Data from this experiment provided the data consistent with a propensity of C99 to form specific homodimers, as previously observed.^{1,14,21–25} Moreover, when homodimerization-induced resonance changes were compared with data in which the dissociation of the C99/CD147-CTD complex was gradually induced by raising the detergent-to-protein ratio, it was possible to establish that heterodimerization is more avid than homodimerization.

Heterodimerization of C99 with CD147-CTD. As summarized in the Introduction, CD147 is found to promote reduced levels of amyloid- β under physiological conditions. However, there has been controversy regarding the mechanism for this phenomenon. While early studies pointed to a direct regulatory role for CD147 in cleavage of C99 by the γ -secretase complex,¹⁰ later studies have disputed this and proposed that CD147 instead lowers amyloid- β levels by promoting extracellular cleavage and clearance of this polypeptide.⁸ The results of this work do not directly address this controversy or provide direct support for either model. However, this work does establish that under micellar model membrane conditions C99 forms a complex with the combined transmembrane and cytosolic domains of CD147. While the affinity associated with formation of this complex appears to be only modest, it could be much higher under native membrane conditions. Affinity under physiological conditions might also be modulated (up or down) by the presence of CD147's ectodomain in the full-length protein and/or by the presence of other interacting proteins. In any case, the conclusion of this work that these two proteins have a propensity to form a complex may prove useful in future studies to fully unravel the relationship of CD147 to the amyloid precursor protein and its downstream proteolytic processing/degradation.

CONCLUSION

The NMR-based approach developed in this work for elucidating the nature of intermolecular interactions between C99 and CD147-CTD should be generally adaptable to numerous other potentially binding pairs of membrane proteins, some of which are of high biomedical significance. For any given pair of proteins, confirmation of specific binding represents a critical first step for further characterization of the complex. For pairs that are found to interact only through nonspecific interactions

or forced cohabitation, the negative results provided by this approach may provide the basis either for pursuit of more optimal model membrane conditions (in which specific binding might take place) or for a timely cessation of unpromising studies.

METHODS

Expression and Purification of C99. Wild-type human C99 with a C-terminal purification tag was expressed in *E. coli* and purified into LMPG micelles as previously described¹ essentially without any modification. To facilitate the acquisition of ^1H – ^{15}N TROSY correlation spectra, ^{15}N enrichment was provided by supplementing M9 minimal medium with 1 g/L $^{15}\text{NH}_4\text{Cl}$ (Sigma, St. Louis, MO). Pure C99 protein was eluted from a Ni–nitrilotriacetic acid (NTA) column using 2–4 column volumes of elution buffer that contained 250 mM imidazole and 0.05% LMPG, pH 7.8. Samples were concentrated using centrifugal filter units (Millipore, Billerica, MA) of 15 000 molecular weight cutoff (MWCO). This ultrafiltration step also concentrates the LMPG in the sample since it has a very low critical micellar concentration and the micelles are much larger than 15 000 Da. Final NMR samples were prepared to be 0.2 mM [^{15}N]C99 in a buffer containing 250 mM imidazole, 1 mM EDTA, and 5% D_2O plus the desired concentration of LMPG at pH 7.4. The LMPG concentrations in stock C99 samples were determined using 1D proton NMR in which the integral of the signal from 5 mM DSS (4,4-dimethyl-4-silapentane-1-sulfonic acid) was used as a concentration standard (see the section below and Supporting Figure 1, Supporting Information).

Expression and Purification of CD147-CTD. The gene encoding CD147-CTD (residues 204–269) was derived from the full-length human gene and amplified by polymerase chain reaction (PCR), including introduction of a *Bam*HI cleavage site at the 3-end and an *Xho*I site at the 5-end. The double-digested PCR product was then ligated into a pET25b *E. coli* expression vector to include a C-terminal hexaHis tag for purification using a Ni–NTA column. The construct was sequenced by the Vanderbilt University DNA sequencing core facility.

For PRE measurement, single cysteine residues were introduced into CD147-CTD, which contains no wild-type cysteines. Mutations were at either 212 (F212C) or 229 (Y229C) using a Qiagen QuickChange mutagenesis kit (Valencia, CA). The cDNAs of CD147-CTD and its single-cysteine mutants were then ligated into expression vectors that were transformed into BL21(DE3) *E. coli* (Novagen, Gibbstown, NJ). A single colony was picked from a Luria broth–agar/ampicillin plate and used to inoculate a 10 mL overnight culture. The overnight culture was then used to inoculate 1 L of Luria broth medium supplemented with 0.1 g/L ampicillin. The cells were grown at 37 °C with vigorous shaking at 225 rpm. CD147-CTD expression was induced by 1 mM isopropyl β -D-1-thiogalactopyranoside (IPTG) when OD_{600} reached 0.8. Cells were harvested by centrifugation after induction for 3–4 h and could then be stored in a -80 °C freezer.

CD147-CTD and its single-cysteine mutants were purified as described for *E. coli* diacylglycerol kinase³⁰ with some modifications. The cell pellet was resuspended in lysis buffer (75 mM Tris, 300 mM NaCl, 0.2 mM EDTA, pH 7.8) at a 20-fold dilution (20 mL of lysis buffer for each gram of cell pellet). To the lysate were added 0.2 mg/mL lysozyme, 0.02 mg/mL of DNase, 0.02 mg/mL RNase, and 5 mM magnesium acetate, followed by the lysate being tumbled at room temperature for 0.5 h. The lysate was then sonicated for 5 min (alternating 5 s on and 5 s off). After sonication, the solution was cooled on ice, and Empigen detergent (Fluka) was added to 3% to extract the protein from the membrane. The lysate was then tumbled at 4 °C for 0.5 h, followed by centrifugation at 20 000 rpm for 20 min to remove debris. The supernatant was then mixed with Qiagen Ni–NTA Superflow resin (1.2 mL

of resin for every gram of cell pellet) which had been pre-equilibrated with buffer A (40 mM HEPES, 300 mM NaCl, pH 7.5). The mixture was tumbled for 0.5 h at 4 °C to maximize the chelating of detergent-solubilized hexaHis-tagged CD147-CTD to the Ni(II) resin. The resin was then transferred to a column and washed with 5 bed volumes of cold Emp/A buffer (40 mM *N*-(2-hydroxyethyl)piperazine-*N'*-ethanesulfonic acid (HEPES), 300 mM NaCl, 3% Empigen, pH 7.5). The resin was then washed with cold buffer B (40 mM HEPES, 300 mM NaCl, 1.5% Empigen, 40 mM imidazole, pH 7.8) until all impurities were eluted, as judged by monitoring A_{280} . The detergent was then exchanged from 1.5% Empigen to 0.05% LMPG by rinsing the column with 12 × 1 bed volumes of cold rinse buffer (25 mM sodium phosphate, 0.05% LMPG, pH 7.5). Finally, CD147-CTD was eluted from the column using elution buffer (250 mM imidazole, 0.05% LMPG, pH 7.8). The purity of the protein was assessed by SDS–PAGE. Usually 15–20 mg of pure protein was obtained from 1 L of Luria–Bertani (LB) culture. CD147-CTD stock solutions used for titrations were then prepared by concentrating the protein to 1.5 mM.

Expression and Purification of KCNE1. In negative control experiments we titrated C99 with human KCNE1, a 129-residue single-span membrane protein that modulates the function of certain potassium channels. KCNE1 and its single-cysteine mutant S64C were expressed and purified as described^{19,31} without any modification. S64C was constructed on the basis of use of a previously constructed cysteine-free KCNE1 mutant (C105A). Final NMR samples were prepared from a stock solution of 1.5 mM KCNE1 in buffer containing 250 mM imidazole, pH 7.4, with the desired level of LMPG.

Determination of Detergent Concentrations. Detergent concentrations required for accurate determination of the mole percent concentration of membrane proteins were determined using 1D proton NMR. The integral of the NMR signal from a known concentration of DSS was used as a concentration reference to which the integral of an LMPG peak can be compared to determine the overall LMPG concentration (Supporting Figure 1A, Supporting Information). To validate this method, we verified the linearity of a plot of the peak integral ratio vs LMPG concentration in a series of samples with fixed (5 mM) DSS concentration and varying LMPG (0.05%, 0.5%, 1%, and 2%; Supporting Figure 1B). For these experiments 32 transients were acquired for each sample using a Bruker 1D proton pulse sequence with water presaturation. The recovery delay was set to 10 s. The same pulse sequence and parameter settings were used for protein samples with unknown LMPG concentrations.

Spin-Labeling of Single-Cysteine Mutant Forms of CD147-CTD and KCNE1. Nitroxide spin-labeling was introduced using a cysteine-specific reaction of the protein with MTSL (Toronto Research Chemicals, Canada). This reaction requires cysteine to be in its reduced state. Therefore, prior to reaction with MTSL, dithiothreitol (DTT) was added to a 2 mM concentration to 0.5 mM protein samples at pH 7.8, followed by incubation at 37 °C for 20–30 min to completely reduce the disulfide bonds. The reduced protein sample was immediately passed through a Bio-Rad Econo-Pac 10 desalting column to remove the DTT and imidazole. The elution buffer contained 25 mM sodium phosphate and 0.05% LMPG at pH 7.8. A 10-fold molar excess (over protein) of MTSL was then added from a 250 mM stock solution in methanol (the latter of which could be stored in the dark and in the freezer under argon). The solution was gently agitated for 1 h at room temperature, followed by 2 h at 37 °C and then overnight incubation at room temperature. In our experience MTSL or residual MTSL-modified DTT has a significant affinity for micelle surfaces, such that buffer exchange using ultrafiltration or a desalting column does not always completely remove the free spin label. Therefore, the spin-labeled protein sample was reloaded onto a Ni–NTA column, followed by extensive washing using 20 bed volumes of 25 mM sodium phosphate and 0.05% LMPG, pH 7.8. The protein was then eluted using 250 mM imidazole and 0.05% LMPG, pH 7.8, and concentrated using Millipore Ultra-15 centrifugal filter units (MWCO 15 000), followed by adjustment of the pH to 7.4.

The spin-labeling efficiency was evaluated by continuous-wave electron paramagnetic resonance (EPR). EPR signals from spin-labeled protein samples were integrated and quantitated through the comparison with the signal integral of 100 μ M TEMPO (2,2,6,6-tetramethylpiperidine-1-oxyl). For Y226C-CD147, the spin-labeling efficiency was >95%, while for F212C-CD147 and S64C-KCNE1, the efficiency was 90%.

Use of NMR To Monitor Protein–Protein Titrations. For all titration experiments, the concentration of [U - ^{15}N]C99 was fixed at 0.2 mM. Final NMR samples were prepared in 250 mM imidazole with the desired concentration of LMPG. The LMPG concentration was adjusted by directly adding LMPG powder or a 10% LMPG stock solution, followed by adjusting the pH to 7.4. All NMR spectra were acquired at 45 °C using a Bruker Avance 600 MHz spectrometer (Bruker Biospin, Germany) equipped with Z-gradient triple-channel cryogenic probe. A sensitivity-enhanced TROSY pulse sequence³² was employed. Spectra were processed using nmrPipe³³ with linear prediction and zero-filling. Peak intensities were obtained using nmrDraw peak-picking followed by nonlinear spectral line shape modeling (nLinLS).³³ To the greatest extent possible, resonance assignments for C99 at pH 7.4 were carried out by correlating peaks with previously assigned peaks for samples at pH 6.5.¹ However, this is possible only for peaks that are in relatively well-resolved parts of the spectra and that do not undergo large pH-dependent shifts.

NMR Measurement of Paramagnetic Relaxation Enhancement. All paramagnetic samples were prepared by mixing 0.2 mM [U - ^{15}N]C99 with spin-labeled CD147-CTD or spin-labeled KCNE1 at the desired ratio. Diamagnetic forms of the same samples were generated by reducing the nitroxide by adding 10 mM ascorbic acid. The LMPG concentration of all samples was 2.5% (ca. 50 mM). 1H – ^{15}N TROSY NMR spectra were acquired using identical parameters for both paramagnetic and the corresponding diamagnetic samples. Each spectrum was processed twice using nmrPipe with either Gaussian or cosine-squared apodization and zero filling. The reported paramagnetic condition to diamagnetic condition peak intensity ratios represent the average of the intensity ratios measured following processing using these alternative apodization functions.

■ ASSOCIATED CONTENT

S Supporting Information. Complete ref 8 and supporting figures illustrating the method used to determine the detergent concentration in NMR samples, the chemical shift changes for C99 induced by titration with CD147 at low LMPG, the chemical shift changes for C99 at a fixed ratio with excess CD147 during titration by LMPG, the chemical shift changes for C99 as it is titrated with LMPG, and the concentration dependence of residue-specific NMR peak line broadening for C99 as it was titrated by spin-labeled CD147 or KCNE1. This material is available free of charge via the Internet at <http://pubs.acs.org>.

■ AUTHOR INFORMATION

Corresponding Author

chuck.sanders@vanderbilt.edu

■ ACKNOWLEDGMENT

This work was supported by Alzheimer Association Grant IIRG-07-59379 and by NIH Grants PO1 GM080513 and U54 GM094608.

■ REFERENCES

- (1) Beel, A. J.; Mobley, C. K.; Kim, H. J.; Tian, F.; Hadziselimovic, A.; Jap, B.; Prestegard, J. H.; Sanders, C. R. *Biochemistry* **2008**, *47*, 9428–9446.

- (2) Buffy, J. J.; Buck-Koehntop, B. A.; Porcelli, F.; Traaseth, N. J.; Thomas, D. D.; Veglia, G. *J. Mol. Biol.* **2006**, *358*, 420–429.
- (3) Kim, M. J.; Park, S. H.; Opella, S. J.; Marsilje, T. H.; Michellys, P. Y.; Seidel, H. M.; Tian, S. S. *J. Biol. Chem.* **2007**, *282*, 14253–14261.
- (4) Malia, T. J.; Wagner, G. *Biochemistry* **2007**, *46*, 514–525.
- (5) Van Horn, W. D.; Kim, H. J.; Ellis, C. D.; Hadziselimovic, A.; Sulistijo, E. S.; Karra, M. D.; Tian, C.; Sonnichsen, F. D.; Sanders, C. R. *Science* **2009**, *324*, 1726–1729.
- (6) Shoichet, B. K.; McGovern, S. L.; Caselli, E.; Grigorieff, N. *J. Med. Chem.* **2002**, *45*, 1712–1722.
- (7) McDonnell, P. A.; Opella, S. J. *J. Magn. Reson., Ser. B* **1993**, *102*, 120–125.
- (8) Vetrivel, K. S.; et al. *J. Biol. Chem.* **2008**, *283*, 19489–19498.
- (9) Zhou, S. X.; Zhou, H.; Walian, P. J.; Jap, B. K. *Drug News Perspect.* **2006**, *19*, 133–138.
- (10) Zhou, S. X.; Zhou, H.; Walian, P. J.; Jap, B. K. *Proc. Natl. Acad. Sci. U.S.A.* **2005**, *102*, 7499–7504.
- (11) Nabeshima, K.; Iwasaki, H.; Koga, K.; Hojo, H.; Suzumiya, J.; Kikuchi, M. *Pathol. Int.* **2006**, *56*, 359–367.
- (12) Winblad, B.; Nahalkova, J.; Volkmann, I.; Aoki, M.; Bogdanovic, N.; Tjernberg, L. O.; Behbahani, H. *Neurochem. Int.* **2010**, *56*, 67–76.
- (13) Steiner, H.; Winkler, E.; Hobson, S.; Fukumori, A.; Dumpelfeld, B.; Luebbers, T.; Baumann, K.; Haass, C.; Hopf, C. *Biochemistry* **2009**, *48*, 1183–1197.
- (14) Wang, H.; Barreyro, L.; Provasi, D.; Djemil, I.; Torres-Arancivia, C.; Filizola, M.; Ubarretxena-Belandia, I. *J. Mol. Biol.* **2011**, *408*, 879–895.
- (15) Khalifa, N. B.; Van Hees, J.; Tasiaux, B.; Huysseune, S.; Smith, S. O.; Constantinescu, S. N.; Octave, J. N.; Kienlen-Campard, P. *Cell Adhes. Migr.* **2010**, *4*, 268–272.
- (16) Zuiderweg, E. R. P. *Biochemistry* **2002**, *41*, 1–7.
- (17) Otzen, D. E.; Sehgal, P.; Mogensen, J. E. *Biochim. Biophys. Acta, Biomembr.* **2005**, *1716*, 59–68.
- (18) Carman, G. M.; Deems, R. A.; Dennis, E. A. *J. Biol. Chem.* **1995**, *270*, 18711–18714.
- (19) Tian, C. L.; Vanoye, C. G.; Kang, C. B.; Welch, R. C.; Kim, H. J.; George, A. L.; Sanders, C. R. *Biochemistry* **2007**, *46*, 11459–11472.
- (20) Van Horn, W. D.; Vanoye, C. G.; Sanders, C. R. *Curr. Opin. Struct. Biol.* **2011**, *21*, 283–291.
- (21) Munter, L. M.; Voigt, P.; Harmeier, A.; Kaden, D.; Gottschalk, K. E.; Weise, C.; Pipkorn, R.; Schaefer, M.; Langosch, D.; Multhaup, G. *EMBO J.* **2007**, *26*, 1702–1712.
- (22) Gorman, P. M.; Kim, S.; Guo, M.; Melnyk, R. A.; McLaurin, J.; Fraser, P. E.; Bowie, J. U.; Chakrabarty, A. *BMC Neurosci.* **2008**, *9*, 17–27.
- (23) Kienlen-Campard, P.; Tasiaux, B.; Van Hees, J.; Li, M.; Huysseune, S.; Sato, T.; Fei, J. Z.; Aimoto, S.; Courtoy, P. J.; Smith, S. O.; Constantinescu, S. N.; Octave, J. N. *J. Biol. Chem.* **2008**, *283*, 7733–7744.
- (24) Sato, T.; Tang, T. C.; Reubins, G.; Fei, J. Z.; Fujimoto, T.; Kienlen-Campard, P.; Constantinescu, S. N.; Octave, J. N.; Aimoto, S.; Smith, S. O. *Proc. Natl. Acad. Sci. U.S.A.* **2009**, *106*, 1421–1426.
- (25) Multhaup, G. *Neurodegener. Dis.* **2006**, *3*, 270–274.
- (26) Battiste, J. L.; Wagner, G. *Biochemistry* **2000**, *39*, 5355–5365.
- (27) Iwahara, J.; Clore, G. M.; Tang, C. *Curr. Opin. Struct. Biol.* **2007**, *17*, 603–616.
- (28) Jahnke, W. *ChemBioChem* **2002**, *3*, 167–173.
- (29) Moore, J. M.; Lepre, C. A.; Peng, J. W. *Chem. Rev.* **2004**, *104*, 3641–3675.
- (30) Oxenoid, K.; Kirn, H. J.; Jacob, J.; Sonnichsen, F. D.; Sanders, C. R. *J. Am. Chem. Soc.* **2004**, *126*, 5048–5049.
- (31) Kang, C. B.; Tian, C. L.; Sonnichsen, F. D.; Smith, J. A.; Meiler, J.; George, A. L.; Vanoye, C. G.; Kim, H. J.; Sanders, C. R. *Biochemistry* **2008**, *47*, 7999–8006.
- (32) Weigelt, J. *J. Am. Chem. Soc.* **1998**, *120*, 10778–10779.
- (33) Delaglio, F.; Grzesiek, S.; Vuister, G. W.; Zhu, G.; Pfeifer, J.; Bax, A. *J. Biomol. NMR* **1995**, *6*, 277–293.